27th EPS Conference on Contr. Fusion and Plasma Phys. Budapest, 12-16 June 2000 ECA Vol. **24B** *(2000) 552 -555*

Studies of H–mode Plasmas Produced Directly By Pellet Injection in the DIII–D Tokamak

P. Gohil,[1] L.R. Baylor,[2] T.C. Jernigan,[2] K.H. Burrell,[1] T.N. Carlstrom,[1] G.R. McKee[3] and T.L. Rhodes[4]

[1]*General Atomics, P.O. Box 85608, San Diego, California 92186-5608, USA*
[2]*Oak Ridge National Laboratory, Oak Ridge, Tennessee, USA*
[3]*University of Wisconsin, Madison, Wisconsin, USA*
[4]*University of California, Los Angeles, California, USA*

A key issue for the physics of H–mode plasmas is to determine which plasma quantities are critical for the formation of the edge transport barrier. One approach is to directly perturb the edge plasma and observe the subsequent changes. In DIII–D, pellet injection has been used to directly change the edge plasma conditions and produce H–mode transitions. One hypothesis for the H–mode transition is that the attainment of a critical edge electron temperature is required for the transition [1–3]. This hypothesis is disproved in this paper. H–mode transitions were produced by injecting frozen deuterium pellets of diameter 2.7 mm from the inner wall of the DIII–D vessel into the high toroidal field side (HFS) and from the outer wall into the low field side (LFS) of the plasma. Both the HFS and LFS pellets produced significant increases in the edge electron density, which led to substantial reductions in the edge electron and ion temperatures. However, H–mode transitions were still produced with the lowered edge temperatures, implying that a critical edge temperature is not necessary for H–mode transitions. The pellet induced H–mode plasma exhibited clear pedestals in electron density and electron and ion temperatures at the plasma edge and persisted for the duration of the applied neutral beam power. The HFS pellet's penetration and deposition profiles were substantially deeper (up to $\rho \approx 0.2$) than that of the LFS pellet (up to $\rho \approx 0.7$). However, since both HFS and LFS pellets produced H–mode transitions, this implies that pellet penetration depth is not important; the important factor is the large increase in the electron density right at the plasma edge produced by both types of pellets. The values of the edge plasma quantities at the H–mode transition were expressed in the parametric terms described in several theories and models of the H–mode transitions [4–6]. On comparison, the experimentally determined parameters at the H–mode transition were well below those required by several theoretical models. Finally, pellet injection reduced the neutral beam power required to produce the H–mode from 7.3 MW to 4.9 MW in plasmas which had the ∇B drift away from the X–point.

These experiments were performed on the DIII–D tokamak with the following ranges of operational parameters: major radius R = 1.67–1.68 m, minor radius a = 0.61–0.62 m, vertical elongation κ = 1.63–1.71, plasma current I_p = 1.6 MA, and toroidal magnetic field strength B_T = 1.8–2.1 T. The plasma configuration was an unbalanced double-null diverted discharge with the vertical drift of the ions being in the $\nabla B \times B$ direction which is away from the dominant X–point. This plasma configuration resulted in a high heating power threshold (>9.2 MW) for the H–mode transition. The pellets were comprised of frozen deuterium with diameters of 2.7 mm. Pellets could be injected at a maximum repetition rate of 10 Hz [7]. Pellets were independently launched from three locations around the DIII–D vacuum vessel (Fig. 1). Pellets were injected horizontally from the outside vessel wall (LFS) at 4 cm above the midplane of the vessel. These LFS pellets were shattered in the guide tube before entry into the DIII–D vessel in order to minimize the pellet penetration in an effort to produce a greater edge density perturbation.

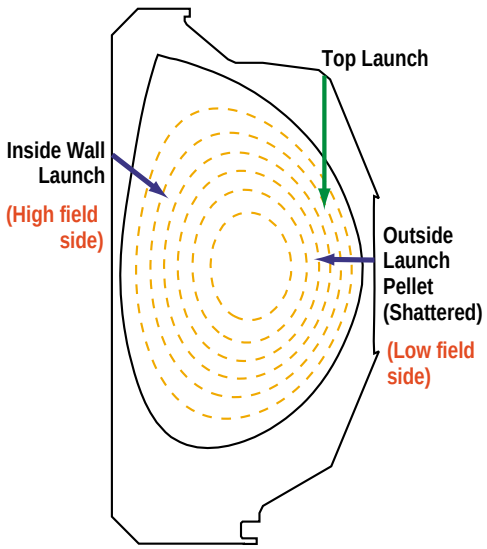

Fig. 1. Pellet launch trajectories with respect to the DIII–D vessel.

Pellets were also separately injected from the inside vessel wall (*i.e.*, HFS) at about 72.1 cm above the vessel midplane and directed downwards towards the plasma center at an angle of 45°. Pellets were also injected vertically downwards into the low field side from an upper port. All three different pellet injection configurations produced H–mode transitions. The pellet velocities varied from about 300 m s^{-1} for the LFS pellets to about 230 m s^{-1} for the HFS pellets.

The application of neutral beam power (P_{NBI} = 9.2 MW) below the H–mode power threshold produced discharges which remained in L–mode throughout the beam heated phase (>700 ms) even in the presence of strong sawteeth. Clearly, the conditions required for the H–mode transition were absent in these plasmas. Figure 2 shows the time evolution of various quantities for a reference discharge without pellets which remained in L–mode at a total input power of 9.5 MW (NBI + ohmic). Also shown is a discharge in which an H–mode transition was directly triggered by pellet injection. Three LFS pellets were injected into this discharge at a reduced total power of7.3 MW. The pellet injection reduced the power threshold by 23%.

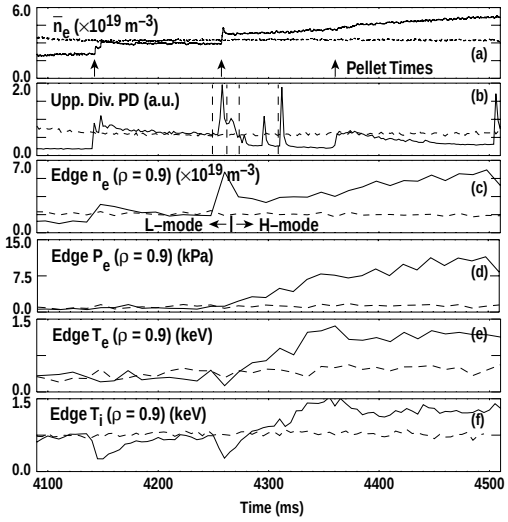

Fig. 2. Time histories of edge quantities for reference discharge with no pellet (shot 99573, dashed line) and PIH–mode discharge (shot 99559, solid line) produced by a LFS launched pellet. Dashed vertical lines in (b) represent times of profiles shown in Fig. 3. n_e = electron density, T_e = electron temperature, P_e = electron pressure, T_i = ion temperature.

The first pellet broke up into two distinct pieces, which then entered the plasma with a time difference of 4 ms. This resulted in a two step and, hence, gradual increase in the edge electron density, n_e, and failed to produce the H–mode transition. However, the second pellet produced a more instantaneous and more significant increase in the edge n_e. The H–mode transition resulted from this more instantaneous edge density perturbation. The edge electron pressure, P_e, increases nearly monotonically after the second pellet injection signifying the formation of the edge transport barrier and the improved confinement in H–mode.

There is a clear decrease in the edge electron temperature, T_e, and ion temperatures, T_i, after pellet injection. The n_e and T_e profiles are determined from Thomson scattering (TS). The T_i profiles are determined from charge exchange recombination (CER) spectroscopy measurements of carbon impurities with a sampling time of 5 ms. The third pellet at 4360 ms is injected into the H–mode plasma edge and leads to a decrease in the edge T_e and T_i. However, the plasma remains steadfastly in H–mode and continues to do so for the next 500 ms. The increase in the divertor photodiode signal at 4360 ms is a result of increased recycling in the scrapeoff layer after the injection of the third pellet and does not represent a return to L–mode conditions since the edge transport barrier is maintained with steep gradients in the edge n_e, T_e, and T_i.

The important dynamics of the PIH–mode transition occur in the region of greatest perturbation by the pellet ($\rho \geq 0.8$). Figure 3 shows detailed profiles of n_e, P_e, T_e, and T_i for $\rho > 0.5$ across the PIH–mode transition. The dashed vertical lines on the time trace of the Balmer-alpha photodiode signal in Fig. 2(b) indicate the times of the TS measurements of n_e, T_e, and P_e. The T_i profiles are shown for the closest times to the TS measurements given that the sampling time of the CER measurements is 5 ms. The pellet produces substantial increases in the n_e (*cf.* to the L–mode profile) in the region $\rho > 0.6$. Correspondingly, in the same region, there are large reductions in the T_e and T_i values. The process appears to be adiabatic since the P_e profile for $\rho > 0.6$ is unchanged. However, the H–mode transition occurs within 12 ms after pellet injection since both the absolute value and gradient of the

edge pressure profile for $\rho \geq 0.9$ have increased significantly by time 4272 ms as a result of the formation of the edge transport barrier. Further, by this time, the electron density between$0.5 < \rho < 0.8$ has also increased substantially from the L–mode value as n_e increases towards the plasma center as a result of the formation of the edge transport barrier. However, by this time, the T_e at $\rho = 0.9$ is at or below the L–mode value and the T_i at $\rho = 0.9$ is well below the L–mode value. This implies that the attainment of a critical edge T_e or T_i is not necessary for H–mode transitions. Furthermore, Fig. 2(e) and 2(f) shows that the reference discharge without pellet injection (dashed line) remained steadfastly in L–mode throughout, despite reaching edge T_e and T_i values even greater than the T_e and T_i observed after pellet injection during the PIH–mode transition.

The large changes in the edge n_e, T_e, and T_i produced by pellet injection provide a direct means of testing theories of the H–mode transition. These theories postulate certain critical threshold parameters for the H–mode transition determined from the local plasma parameters and their gradients in the plasma edge. The high spatial resolution of the relevant edge diagnostics on DIII–D provide the necessary measurements to make these comparisons with the theories. Figure 4 shows the comparisons between experimental results and the formulated threshold parameters postulated by three theories of the H–mode transition. Figure 4(a) is a comparison with the model of Rogers and Drake [4] which is based on 3–D simulations of the Braginskii equations where the H–mode threshold requirements is parameterized in terms of the edge MHD ballooning parameter α_{MHD} and a diamagnetic parameter α_{DIA}.The model is for a shifted circle magnetic geometry, but the equations have been modified for a close approximation to the shaped discharges in DIII–D. In their model, transport is suppressed when $\alpha_{MHD} \gtrsim 0.5$ and $\alpha_{DIA} \gtrsim 0.5$ in DIII–D. This then defines the parametric region for access to the H–mode (shaded region). The experimental points are evaluated at the location of the maximum edge density gradient and, hence, pressure gradient which gives the highest value for α_{MHD} for the various points. The injection of the pellet greatly increases the collisionality and, hence, lowers the α_{DIA} parameter. After the H–mode transition, the increased temperatures lead to increases in the edge pressure (increased α_{MHD}) and to lower edge collisionality (increased α_{DIA}). Also shown is the experimental point well into the H–mode and just before a giant ELM. These conditions are in closer agreement to the model requirements, but represent well established H–mode values by which time the edge pressure gradients have increased substantially.

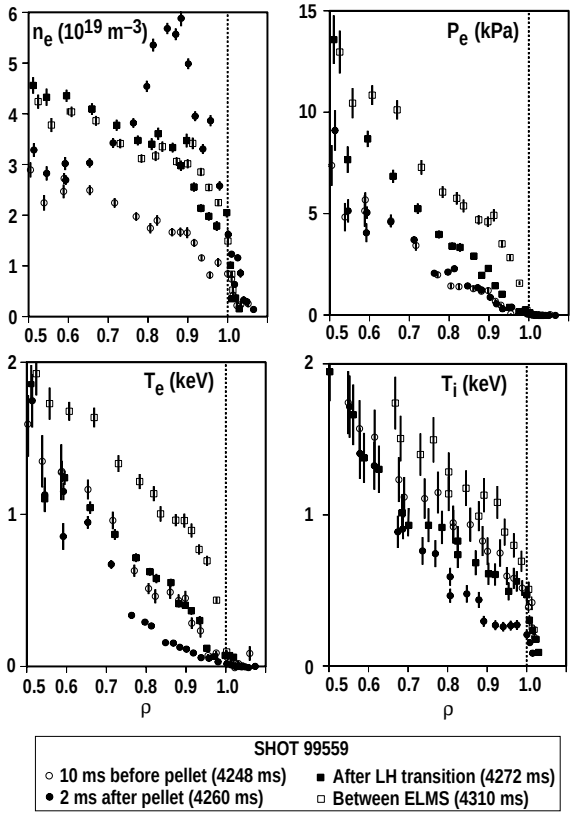

Fig. 3. n_e, P_e, T_e, and T_i radial profiles across the PIH–mode transition for the H–mode shot in Fig. 2. The dashed vertical line in the profile plots represent the location of the separatrix.

In another model of the H–mode transition by Pogutse *et al.*, [5] an increased plasma pressure leads to the Alfvén waves mixing with the electron drift waves and stabilizing the long wavelength turbulence. Their Alfvén drift model predicts that turbulent transport is suppressed when $\beta_n > 1 + \nu_n^{2/3}$, where β_n and ν_n are the edge normalized beta and normalized collision frequency, respectively. This inequality is satisfied for the shaded region in Fig. 4(b) and represents the requirements for H–mode. The experimental values for β_n and ν_n are well below the model predictions for all points up to and through the H–mode transition.

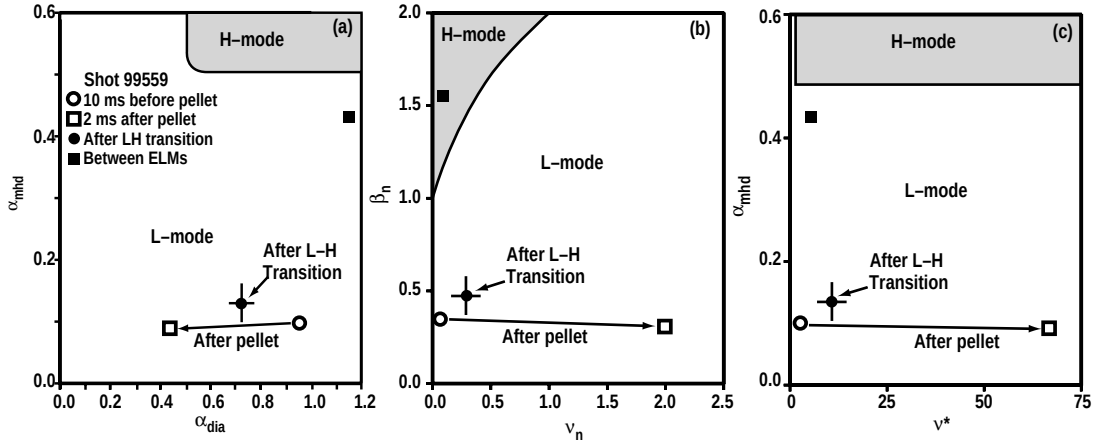

Fig. 4. Comparison of experimental edge local parameters with predictions from theories of the H–mode transitions. (a) cf. with theory of Rogers and Drake [4]; (b) cf. with theory of Pogutse et al. [5]; (c) cf. with theory of Wilson, et al. [6].

In another model of the H–mode transition, unstable peeling modes at low edge collisionality are invoked by Wilson *et al.*, [6] to explain the increased difficulty in obtaining H–mode transitions at low edge collisionality in the COMPASS–D tokamak. At higher edge collisionality ($\nu^* > 1$), the peeling mode can be stabilized by increasing the edge pressure gradient, *i.e.*, $\alpha_{MHD} \gtrsim 0.5$ and $\nu^* \gtrsim 1$. This parameter space for reduced transport and improved confinement is shown in Fig. 4(c). Once again, the experimental edge pressure gradient at the H–mode transition is far below the theoretical predictions even for edge pressure gradients well into the H–mode phase. All the models have a requirement for the edge pressure gradient at the H-mode transition which is greatly overestimated when compared with the experimental values.

PIH–mode transitions are not dependent on the pellet penetration and deposition depths in the plasma. This conclusion is based on observation of H–mode transitions both with HFS and LFS injection, which produce very different deposition profiles. The HFS pellet descriptions were much deeper (to $\rho \sim 0.2$) than the LFS pellet's depositions (to $\rho \sim 0.8$). However, both forms of pellet injection produced very steep edge density gradients. It appears that the degree of particle deposition depth is not important; the important feature is the production of a steep density gradient at the plasma edge. One postulate for the PIH–mode transition is that the steep edge density gradient can lead to changes in the edge main ion pressure gradient and the edge toroidal and poloidal rotation (through drag from the increased particle density). These can then result in increased shear in the edge radial electrical field, E_r, and E×B shearing rate, $\omega_{E\times B}$, leading to an H–mode transition. Edge E_r determined from CER across the pellet injection shows that $\omega_{E\times B}$ changes from $2 \times 10^5\ s^{-1}$ to $5 \times 10^5\ s^{-1}$, which is consistent with the idea that changes in E×B shear produce the transition [8]. Further experiments are planned to determine causality by making measurements of the edge E_r across the PIH–mode transition at 1 to 2 ms time resolution using the DIII–D CER system.

This is a report of research sponsored by the U.S. Department of Energy under Contract Nos. DE-AC03-99ER54463 and DE-AC05-00OR22725.

[1] ASDEX Team, Nucl. Fusion **29**, 1959 (1989).
[2] F. Ryter *et al.*, Plasma Physics and Controlled Fusion **40**, 725 (1998).
[3] A. Hubbard *et al.*, Plasma Physics and Controlled Fusion **40**, 689 (1998).
[4] B. N. Rogers and J. F. Drake, Phys. Rev. Lett. **81**, 4396 (1998).
[5] O. Pogutse *et al.*, *Proceedings of the 24th European Conference on Controlled Fusion and Plasma Physics, Berchtesgaden, 1997* (European Physical Society, Petit-Lancy, 1997) Vol. 21A, Part III, p. 1041.
[6] H. R. Wilson *et al.*, Phys. Plasmas **6**, 1925 (1999).
[7] L. R. Baylor *et al.*, Fusion Tech. **34**, 425 (1998).
[8] K.H. Burrell, Phys. Plasmas **4**, 1499 (1997).